

Modelling excess properties of mineral and melt solutions over large P-T ranges: implications for phase relations and seismic velocities in the mantle

R. Myhill

Bayerisches Geoinstitut, Universität Bayreuth, Universitätsstrasse 30, 95447 Bayreuth, Germany

Abstract

Thermodynamic models of solid and liquid solutions in the Earth Sciences are increasingly used to calculate phase relations and seismic properties over large pressure and temperature ranges. Calculations often span over 1000 K and 5 GPa in studies of exhumation processes and metamorphism in subduction zones. Research into mantle phase relations and differentiation of the early Earth frequently involves calculations over 3000 K and 100 GPa. Despite spanning such huge ranges, a common approximation is that excess thermodynamic derivatives within solid solutions (entropy and volume) are constant with respect to pressure and temperature. This is generally not true; absolute excess volumes tend to decrease with increasing pressure. As a result, the constant volume approximation may have a significant effect on both phase relations and seismic velocities calculated from solid solution models.

In this paper, we present a solution to this problem by extending the sub-regular Margules mixing model using intermediate compounds to define the thermodynamic properties of solid solutions. Mathematical derivations are provided for excess properties (H^{ex} , S^{ex} , V^{ex}) and their pressure and temperature derivatives (K_T^{ex} , α^{ex} , Cp^{ex} etc.). We provide examples of pyroxene, garnet and melt solutions, showing that inclusion of a variable excess volume is vital

*Corresponding author: R. Myhill
Email address: myhill.bob@gmail.com (R. Myhill)

to simulate observed phase relations and seismic velocities. Heuristics are suggested for intermediate compounds where individual thermodynamic properties are poorly constrained.

Keywords: high pressure, excess properties

1. Introduction

Solution models are a vital part of estimating phase relations in the Earth. Typically, some functional form (often quadratic, cubic) is used to describe excess non-configurational energies between endmembers. Where necessary, the
5 parameters describing the properties of the solid solution are allowed to vary as a function of pressure and temperature.

$$W_{ij} = W_{ij}^H + W_{ij}^V P + W_{ij}^S T \quad (1)$$

Models described in this way have been extremely successful in describing the properties of solid solutions up to pressures of a few GPa. Increasingly, such models are being used over larger and larger pressure ranges. For example,
10 garnet models are now being used to estimate phase relations in the mantle transition zone, and models of metallic alloys and melts are being used to study the composition and evolution of the Earth's core. Solution models are also increasingly being used to estimate seismic velocities in the mantle and core. These two developments present a problem for the traditional approach to es-
15 timating mixing properties, because they are both strongly dependent on the change in excess volume with pressure, a variable which is identical to zero in Equation 1.

To explain in a simple way why excess volumes are likely to change with pressure, imagine two crystal lattices (A_xO_y and B_xO_y) comprising cations
20 with different ionic radii and field strengths. The properties of the cations (and anion) result in different unit cell volumes and compressibilities; typically the lattice with the larger cationic radius will have a large volume and smaller bulk modulus (Anderson and Anderson, 1970). Now imagine a third lattice

with intermediate composition ($[A_{1-z}B_z]_xO_y$). This lattice will typically exhibit
25 distortions which result in a positive or negative excess volume, as a direct result
of changing the average cation-anion bond length relative to the sum of the
endmembers (Vegard’s Law). It is reasonable to suggest that longer bonds will
be more compressible, and that therefore a positive excess bulk modulus will
result in a negative excess bulk modulus. The reverse is also true; shorter bonds
30 are likely to be less compressible. Of course, compression in complex minerals
is unlikely to be well-described by a simple isotropic change in bond length.
Nevertheless, other compression mechanisms such as polyhedral rotation are
likely to be affected in a similar way; in general, a smaller volume will reduce
the flexibility of the structure.

35 There is currently no formulation to model solid solutions in the case that
constant excess volumes (or indeed excess entropies) are an inappropriate ap-
proximation. We introduce here a simple adaptation of the subregular Margules
mixing model, using intermediate compounds to describe the excess properties
of the solid solution as a function of pressure and temperature. The added flex-
40 ibility comes with a large increase in the number of free parameters, so we also
provide useful heuristics for the cases where individual parameters are unknown.

The new form of the model is illustrated with the use of three implemen-
tations for pyroxene, garnet and Fe-FeO melt. We show that for these cases a
constant excess volume based on room pressure data is a bad approximation
45 beyond a few GPa pressure, and errors in seismic velocities and phase relations
result from not incorporating reasonable decays in excess volume. This new
formulation should enable a large number of studies on elastic properties of
solid solutions to be incorporated into thermodynamic models. The study also
highlights the need for high quality equation of state data for intermediate com-
50 positions within solid solutions; data which is currently lacking, even in systems
with sizeable excess volumes.

2. The Extended Subregular Margules (ESM) model

The subregular Margules mixing model within a binary system A - B approximates excess Gibbs free energies at any given pressure and temperature as a cubic function of composition (Helffrich and Wood, 1989):

$$\mathcal{G}^{xs} = X_B(1 - X_B)(W_{AB}X_B + W_{BA}(1 - X_B)) \quad (2)$$

In the special case that $W_{AB} = W_{BA}$, the function is a quadratic. We can define the Gibbs interaction parameter in terms of the Gibbs free energy of a 50:50 intermediate compound (AB) and the endmembers A and B :

$$W_{AB}^{\mathcal{G}} = 4(\mathcal{G}_{AB} + T\mathcal{S}_{AB}^{\text{conf}}) - 2(\mathcal{G}_A + \mathcal{G}_B) \quad (3)$$

where $\mathcal{S}_{AB}^{\text{conf}}$ is the configurational entropy of the intermediate compound. In the more general case that $W_{AB} \neq W_{BA}$, Equation 2 can be thought of as two symmetric interaction parameters with contributions that depend on the composition. Two intermediate compounds (AB and BA) are then required to describe the properties of the solution (Figure 1).

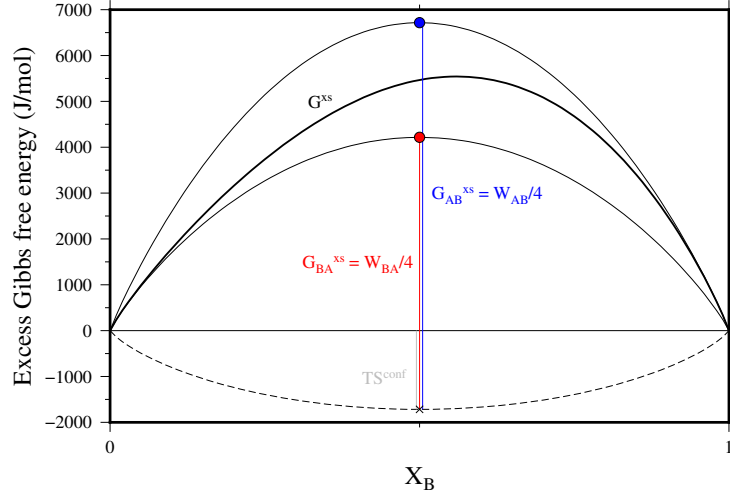


Figure 1: Schematic illustration of a binary subregular solution model.

Expanding the subregular solution model beyond a binary system, the excess

65 nonconfigurational Gibbs free energy is (Helffrich and Wood, 1989)

$$\mathcal{G}^{xs} = \sum_{i=1}^n \sum_{j>1}^n X_i X_j \left(W_{ij} X_j + W_{ji} X_i + 0.5(W_{ij} + W_{ji}) \sum_k^n (1 - \delta_{ik})(1 - \delta_{jk}) X_k \right) \quad (4)$$

Each of the individual W_{ij} terms in Equation 4 can be determined via the properties of an intermediate compound, just as described in the binary A - B system (Equation 2). The properties of the solid solution with composition X_i are then defined as follows:

$$\mathcal{G} = \sum_i X_i \mathcal{G}_i + \mathcal{G}^{xs} \quad (5)$$

$$\mathcal{H} = \sum_i X_i \mathcal{H}_i + \mathcal{H}^{xs} \quad (6)$$

$$\mathcal{S} = \sum_i X_i \mathcal{S}_i + \mathcal{S}^{xs} \quad (7)$$

$$\mathcal{V} = \sum_i X_i \mathcal{V}_i + \mathcal{V}^{xs} \quad (8)$$

$$C_P = \sum_i X_i C_{P,i} + T \left(\frac{\partial \mathcal{S}}{\partial T} \right)_P^{xs} \quad (9)$$

$$\alpha = \frac{1}{\mathcal{V}} \left(\sum_i X_i \alpha_i \mathcal{V}_i + \left(\frac{\partial \mathcal{V}}{\partial T} \right)_P^{xs} \right) \quad (10)$$

$$K_T = \frac{\mathcal{V}}{\sum_i \frac{X_i \mathcal{V}_i}{K_{T,i}} - \left(\frac{\partial \mathcal{V}}{\partial P} \right)_T^{xs}} \quad (11)$$

$$C_V = C_P - \mathcal{V} T \alpha^2 K_T \quad (12)$$

$$K_S = K_T \frac{C_P}{C_V} \quad (13)$$

$$\gamma = \frac{\alpha K_T \mathcal{V}}{C_V} \quad (14)$$

70 With the exception of the enthalpy excess, excess terms (\mathcal{S}^{xs} , \mathcal{V}^{xs} etc) are derived in the same way as the excess Gibbs free energy (Equation 4), with interaction terms defined as follows:

$$W_{ij}^{\mathcal{S}} = 4(\mathcal{S}_{ij} - \mathcal{S}_{ij}^{\text{conf}}) - 2(\mathcal{S}_i + \mathcal{S}_j) \quad (15)$$

$$W_{ij}^{\mathcal{V}} = 4\mathcal{V}_{ij} - 2(\mathcal{V}_i + \mathcal{V}_j) \quad (16)$$

$$W_{ij}^{\partial\mathcal{V}/\partial P} = -4\mathcal{V}_{ij}/K_{Tij} + 2(\mathcal{V}_i/K_{Ti} + \mathcal{V}_j/K_{Tj}) \quad (17)$$

$$W_{ij}^{\partial\mathcal{V}/\partial T} = 4\alpha_{ij}\mathcal{V}_{ij} - 2(\alpha_i\mathcal{V}_i + \alpha_j\mathcal{V}_j) \quad (18)$$

$$W_{ij}^{\partial\mathcal{S}/\partial T} = \frac{4C_{Pij} - 2(C_{Pi} + C_{Pj})}{T} \quad (19)$$

Finally, excess enthalpy is defined as

$$\mathcal{H}^{xs} = \mathcal{G}^{xs} + T\mathcal{S}^{xs} \quad (20)$$

2.1. Heuristics

75 It is often the case that endmembers are particularly well studied, while the properties of the solid solution are constrained only by enthalpies of solution and volumes at room temperature and pressure. The remaining properties of the intermediate compounds must be estimated by the user. In this study, we suggest that the following heuristics be used:

$$\mathcal{S}_{ij} = 0.5(\mathcal{S}_i + \mathcal{S}_j) + \mathcal{S}_{ij}^{\text{conf}} \quad (21)$$

$$C_{Pij} = 0.5(C_{Pi} + C_{Pj}) \quad (22)$$

$$\alpha_{ij} = 0.5\mathcal{V} \left(\frac{\alpha_i}{\mathcal{V}_i} + \frac{\alpha_j}{\mathcal{V}_j} \right) \quad (23)$$

$$K'_T = -\frac{\partial}{\partial P} \left(\mathcal{V} \left(\frac{\partial P}{\partial \mathcal{V}} \right)_T \right) \sim \mathcal{V} \left(\sum_i \frac{X_i \mathcal{V}_i}{K'_{Ti} + 1} \right)^{-1} - 1 \quad (24)$$

80 If excess volumes are zero, it is likely that they will remain zero as temperatures and pressures increase. In this case, the bulk modulus is given by Equation 11, with the differential term equal to zero. In contrast, non-zero excess volumes are unlikely to remain constant with pressure and temperature. We suggest that, in the absence of other data a useful heuristic is $(\frac{\partial \mathcal{V}}{\partial P})_T^{xs} \rightarrow 0$
85 as $P \rightarrow \infty$.

A useful way to view the change in bulk modulus across a solid solution is to compare the excess bulk modulus to that implied by the $K_T V = \text{constant}$ rule of thumb proposed by Anderson and Anderson (1970) to estimate the compressibility of endmembers based on their molar volumes. The heuristic we propose

90 in this study predicts a larger excess term than that suggested by the rule of thumb, which we describe using a factor ξ :

$$K_T \sim 0.5(K_{Ti} + K_{Tj}) + \xi \left(\frac{K_{Ti}\mathcal{V}_j + K_{Tj}\mathcal{V}_i}{2\mathcal{V}} - 0.5(K_{Ti} + K_{Tj}) \right) \quad (25)$$

Typically, a value of ~ 6 provides a useful estimate of ξ .

Now that we have described the new model and heuristics related to the construction of intermediate compounds, we turn to a few geologically relevant
 95 examples. The models in this study are all implemented in the open software *burnman*, a mineral physics toolkit written in python. The software, first described in Cottaar et al. (2014), was originally designed for seismic velocity calculations. It has since been augmented with thermodynamics functionality, including a range of different models for solid solutions.

100 3. Examples

3.1. Pyroxene

Our first example is that of jadeite-aegirine pyroxene, an almost ideal solid solution (from a volumetric perspective). We use this model to illustrate that even when excess volumes are extremely small, excess bulk moduli are resolvable.
 105 The experimental data is that of Nestola et al. (2006), and the equation of state used is the Modified Tait (Holland and Powell, 2011). The fit to the volume data is shown in Figure 2.

Table 1: Jadeite-Aegirine mixing parameters to fit the room temperature data of Nestola et al. (2006). The K'_0 for the intermediate compound is fixed to the value given by the heuristic proposed in the text. $K''_0 = -K'_0/K_0$.

	jadeite	aegirine	jd ₅₀ ae ₅₀	ae ₅₀ jd ₅₀
V_0 (cm ³ /mol)	60.5640 \pm 0.0001	64.6261 \pm 0.0004	62.3641 \pm 0.0005	62.4522 \pm 0.0005
K_0 (GPa)	133.5 \pm 0.2	116.0 \pm 0.2	124.8 \pm 0.5	126.7 \pm 0.4
K'_0	4.6 [fixed]	4.4 [fixed]	4.4785 [heuristic]	4.4785 [fixed]

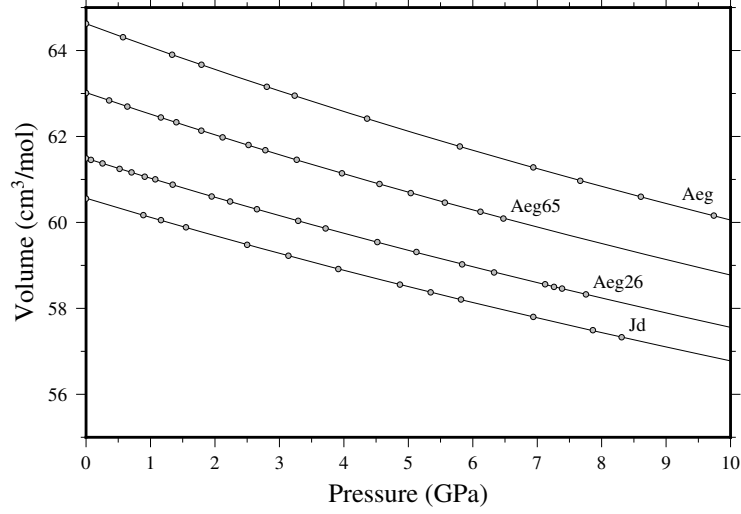


Figure 2: Pressure-volume data in the binary system Jadeite-Aegirine (Nestola et al., 2006), with the model proposed in this study.

Using the derived properties of the solid solution, we can fit the excess volume as a function of pressure (Figure 3). The decay of excess volume as a function of pressure is in excellent agreement with the prediction that excess volumes decay to zero at extreme pressures. For the 50:50 intermediate, our excess bulk moduli and volumes indicate that $\xi \sim 11$ (Equation 25).

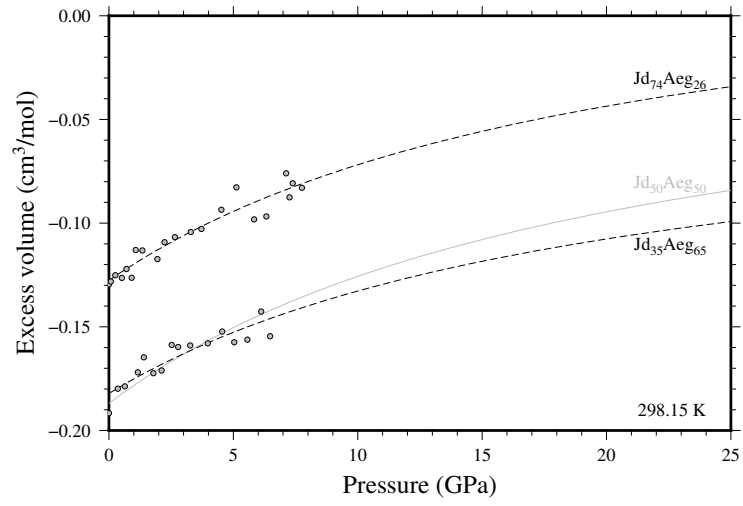


Figure 3: Excess volume for Jd-Aeg pyroxenes calculated from our model.

3.2. Garnet

Our second example is the pyrope-grossular join, which is well-known to have
115 significant non-ideality and volumes of mixing (Newton et al., 1977; Bosenick
and Geiger, 1997; Ganguly et al., 1996). Recently, it has been suggested that
the excess volumes of mixing are $\sim 1 \text{ cm}^3/\text{mol}$, 2–3 times larger than previously
suggested, and associated with very large negative excess bulk moduli (Du et al.,
2015). It is proposed that the differences are due to a hydrogrossular component
120 in the crystals synthesised in piston cylinder apparatus in earlier studies, which
becomes unstable at high pressures.

Here, we create four models to describe the room temperature equations of
state for the pyrope-grossular system using the pyrope and grossular endmem-
bers from Holland and Powell (2011). Two models are presented for the data
125 of (Du et al., 2015), to describe the reported behaviour close to the center and
at the edges of the solid solution. The third model is the constant volume sub-
regular Margules model of Ganguly et al. (1996). A fourth model has the same
excess volume as Ganguly et al. (1996), but a negative excess bulk modulus
which allows the excess volume to decay to zero at high pressures ($\xi = 6$). The
130 standard state bulk moduli are shown in Figure 4.

It is immediately obvious that the bulk moduli calculated from the Du et al.
(2015) study exhibit very large deviations from a linear trend. The symmetric
curve derived from the two compounds in the middle of the binary yields $\xi = 10$,
a value which is not unreasonable, and results in a change in sign of the volume
135 excess at 20–25 GPa. In contrast, the trend derived from the compounds with
20% and 80% pyrope content yields $\xi = 52$. This extreme value leads to negative
excess volumes at 5–6 GPa, which does not seem to be very likely. To avoid
this, K_T' must be increased to >20 , which is also extremely unlikely.

The trend calculated from the terms in Ganguly et al. (1996) has a small
140 positive excess bulk modulus, which is always the case where \mathcal{V}^{xs} is held fixed.
For the reasons outlined in the introduction, this is probably unlikely. The final
model, constructed using the heuristics described in the previous section yields
an excess bulk modulus on the order of 2–3 GPa.

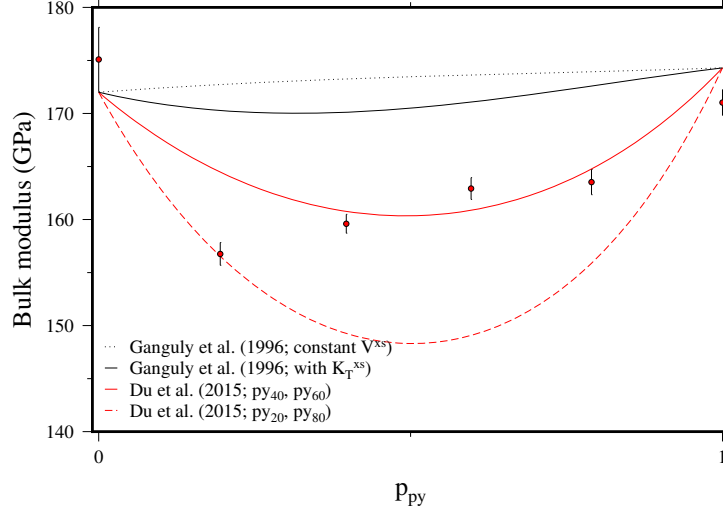


Figure 4: Bulk moduli in the binary system Pyrope-Grossular (Du et al., 2015), with the models proposed in this study.

These models are now used to illustrate the effect of decaying excess vol-
 145 umes on seismic wave velocities. P-wave, S-wave and bulk sound velocities are
 functions of isentropic bulk and shear moduli and density:

$$V_P = \sqrt{\frac{K_S + \frac{4}{3}G}{\rho}} \quad (26)$$

$$V_S = \sqrt{\frac{G}{\rho}} \quad (27)$$

$$V_\Phi = \sqrt{\frac{K_S}{\rho}} \quad (28)$$

Thermodynamic solution models say nothing about shear moduli, so we restrict
 our discussion to the bulk sound velocity. Figure 5 shows the bulk sound velocity
 at ambient temperature for the four solid solution models in the text. The
 150 models of Du et al. (2015) result in large depressions of bulk sound velocity. The
 model constructed from the py₄₀ and py₆₀ samples results in a 4% depression
 relative to the constant \mathcal{V}^{xs} case throughout the upper mantle pressure range.
 In contrast, the model based on the excess volume model proposed in Ganguly
 et al. (1996) predicts a 1% decrease in bulk sound speed.

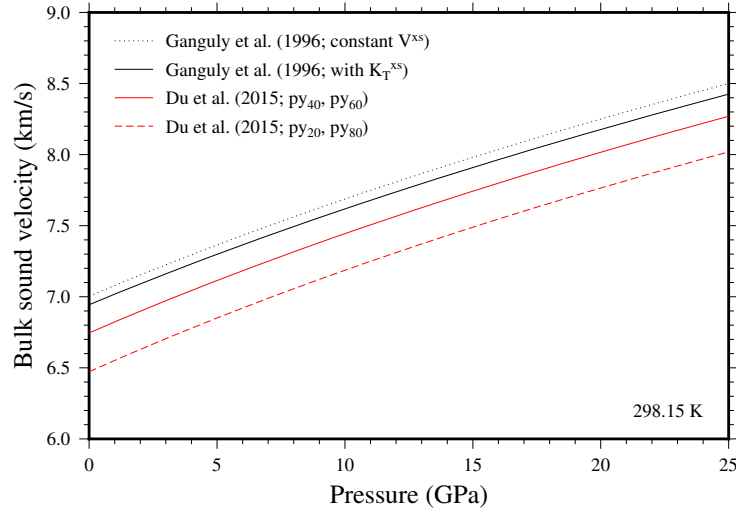


Figure 5: Bulk sound velocities of $\text{Py}_{50}\text{Gr}_{50}$ at room temperature according to the fixed excess volume model of (Ganguly et al., 1996), a modified model incorporating an excess bulk modulus, and the two models derived from Du et al. (2015).

At present, it is not easy to state with certainty whether natural garnets have P-V-T equations of state similar to those suggested by Du et al. (2015), or similar to those in previous studies (Newton et al., 1977; Bosenick and Geiger, 1997; Ganguly et al., 1996). If a hydrogrossular component is indeed the cause for low excess volumes in piston cylinder-synthesised garnets, then garnets in the mantle are likely to have relatively high volume excesses and low bulk moduli. In this case, constant V^{xs} models are clearly inappropriate both for calculations of mantle phase relations and seismic velocities. Nevertheless, even in the case of the model derived from Ganguly et al. (1996), phase relations are still likely to be affected noticeably by the change in excess volume with pressure. At the conditions where garnet finally breaks down, the differences in free energy between models are on the order of kilojoules. Accurately constraining the elastic properties of solid solutions should be a key goal both for seismic velocity calculations and for thermodynamics.

3.3. Fe-FeO melt

Our final example is that of Fe-FeO melt. As oxygen may be one of the more abundant light elements in the core, understanding the thermodynamics of this liquid solution is an important part of understanding mantle-core differentiation and interaction over billions of years. At pressures <25 GPa, the Fe-FeO solution exhibits significant non-ideality, with a large miscibility gap between ionic and metallic Fe-O liquids (Kowalski and Spencer, 1995; Tsuno et al., 2007; Frost et al., 2010). As pressure increases, this miscibility gap disappears, indicating a negative excess volume of mixing (Figure 6). To explain the increase in eutectic temperature with pressure, Komabayashi (2014) suggest that mixing becomes essentially ideal at >100 GPa.

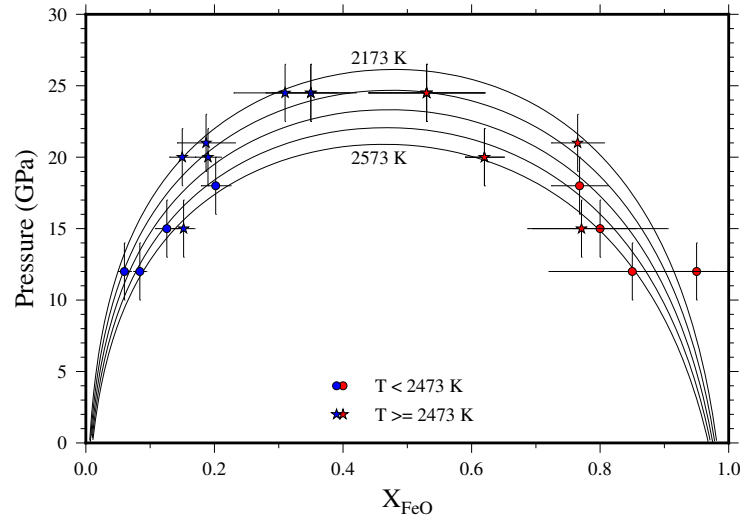


Figure 6: Fe-O solvus

To model processes of mantle differentiation and core formation, it would be extremely useful to have a single model describing the properties of melts over relevant pressure and temperature ranges. Clearly a high pressure ideal model cannot be reconciled with a low pressure model with large excess volumes of mixing without incorporating excess bulk moduli and thermal expansivities. Below ~ 25 GPa, the properties of the liquid can be estimated using the compositions

of coexisting metallic and ionic liquid (Tsuno et al., 2007; Frost et al., 2010). The chemical potentials of Fe and FeO are equal in the ionic and metallic liquids, providing the two constraints necessary to estimate Margules parameters at each pressure and temperature (Figure 7).

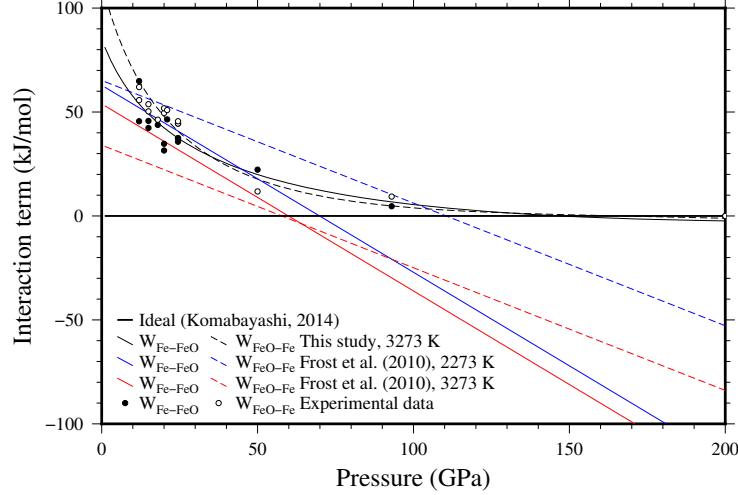


Figure 7: Interaction terms in Fe-FeO melt as a function of pressure.

At >25 GPa, the pressure, temperature and compositions of eutectic liquid at high pressure (Seagle et al., 2008) provide further constraints, providing we know the relative Gibbs free energies of liquid and solid Fe and FeO. Here, we fit the thermodynamic properties of the FCC and HCP iron endmembers and of B1 FeO to published P-V-T data and phase boundaries. The liquid endmembers are fit with available room pressure data, and the effect of pressure is estimated using constraints on the melting curves from Anzellini et al. (2013), Seagle et al. (2008) and Ozawa et al. (2011). The uncertainties on composition and temperature of the eutectic are rather large, so these data are supplemented by the requirement that excess volumes become zero at very high pressure. The parameters used to create the fits in Figures 7 and 8 are given in Table 2. In this work, we fix excess entropy and thermal expansion to zero. The majority of the <25 GPa data was collected within a ~ 200 K temperature range, and is associated with similar temperature uncertainties, which introduces very large uncertainties in

excess entropies. Add to that the possibility of phase separation during quench
 205 and the large uncertainty in coexisting ionic/metallic melt compositions, there
 is no clear evidence for the large temperature dependence proposed by Frost
 et al. (2010), although they do slightly improve the fit to the data (mostly by
 increasing the pressure at which the solvus closes at high temperature).

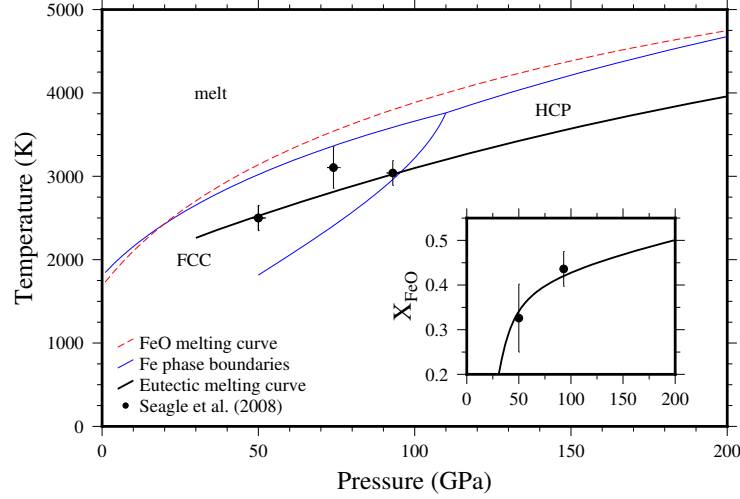


Figure 8: Melting temperature in the Fe-O system as a function of pressure. Inset: eutectic composition in the Fe-O system.

Table 2: Excess Fe-FeO mixing parameters to fit the data in Figures 7 and 8 at a reference temperature of 1809 K and pressure of 50 GPa.

Property	$\text{Fe}_{50}\text{FeO}_{50}$	$\text{FeO}_{50}\text{Fe}_{50}$
H^{xs} (J/mol)	5000 ± 400	4400 ± 400
S^{xs} (J/K/mol)	0 [fixed]	0 [fixed]
V^{xs} (cm^3/mol)	-0.117 ± 0.009	-0.136 ± 0.009
K^{xs} (GPa)	28 ± 5	45 ± 5
K'^{xs}	-0.07 ± 0.12	-0.37 ± 0.12
a^{xs}	0 [fixed]	0 [fixed]

4. Discussion

210 The use of intermediate compounds to describe excess properties is an extremely simple but powerful concept that lends a great deal of flexibility to models without necessarily increasing the number of parameters which need to be fit to the available experimental data. We note that the equations derived here are all quite general, and therefore easily applicable to a wide range of
215 different equations of state.

The heuristics suggested here place constraints on seismic properties which are significantly more strict than typical uncertainties on bulk moduli derived from ultrasonic interferometry, Brillouin scattering or static compression. For example, along the pyrope-majorite join, excess volumes are small ($0.1 \text{ cm}^3/\text{mol}$)
220 (Heinemann et al., 1997). With the assumption that excess volumes decrease to zero with increasing pressure, the excess bulk modulus is constrained to be ~ 0.6 GPa. In comparison, the range in bulk modulus estimates anywhere along the pyrope-majorite join is about 10 GPa (see, for example Hunt et al., 2010). So far, high pressure elasticity studies have mostly been focussed on binary joins
225 with small excess volumes at ambient pressure (Fan et al., 2015; Huang and Chen, 2014). That they should exhibit small excess bulk moduli is in excellent agreement with the heuristics proposed here, but a far more rigorous test would be to investigate systems with large volume excesses.

It is envisaged that the model formulation proposed in this study will be very
230 useful in modelling silicate and metallic melts, where excess volumes are large at low pressure. Even in the MgO-SiO_2 system, excess entropies and volumes are strongly dependent on temperature and pressure (de Koker et al., 2013). Finally, this model allows for much greater freedom in adjusting the shapes of free energy curves as a function of pressure and temperature, which should
235 be extremely useful for phase equilibria studies, especially those investigating chemical potentials and fugacities which depend greatly on the compositional gradient of the free energy curve.

5. Acknowledgments

RM is funded by the Advanced ERC Grant awarded to the “ACCRETE”
240 project.

References

- Anderson, D.L., Anderson, O.L., 1970. Brief report: The bulk modulus-volume relationship for oxides. *Journal of Geophysical Research* 75, 3494–3500.
- Anzellini, S., Dewaele, A., Mezouar, M., Loubeyre, P., Morard, G., 2013. Melt-
245 ing of Iron at Earth’s Inner Core Boundary Based on Fast X-ray Diffraction. *Science* 340, 464–466.
- Bosenick, A., Geiger, C.A., 1997. Powder x ray diffraction study of synthetic pyrope-grossular garnets between 20 and 295 k. *Journal of Geophysical Research: Solid Earth* 102, 22649–22657.
- 250 Cottaar, S., Heister, T., Rose, I., Unterborn, C., 2014. BurnMan: A lower mantle mineral physics toolkit. *Geochemistry, Geophysics, Geosystems* 15, 1164–1179.
- de Koker, N., Karki, B.B., Stixrude, L., 2013. Thermodynamics of the MgO-SiO₂ liquid system in Earth’s lowermost mantle from first principles. *Earth
255 and Planetary Science Letters* 361, 58–63.
- Du, W., Clark, S.M., Walker, D., 2015. Thermo-compression of pyrope-grossular garnet solid solutions: Non-linear compositional dependence. *American Mineralogist* 100, 215–222.
- Fan, D., Xu, J., Ma, M., Liu, J., Xie, H., 2015. Pvt equation of state of
260 spessartinealmandine solid solution measured using a diamond anvil cell and in situ synchrotron x-ray diffraction. *Physics and Chemistry of Minerals* 42, 63–72.
- Frost, D.J., Asahara, Y., Rubie, D.C., Miyajima, N., Dubrovinsky, L.S., Holzapfel, C., Ohtani, E., Miyahara, M., Sakai, T., 2010. Partitioning of
265 oxygen between the Earth’s mantle and core. *Journal of Geophysical Research (Solid Earth)* 115, 2202.

- Ganguly, J., Cheng, W., Tirone, M., 1996. Thermodynamics of aluminosilicate garnet solid solution: new experimental data, an optimized model, and thermometric applications. *Contributions to Mineralogy and Petrology* 126, 137–151.
- Heinemann, S., Sharp, T.G., Seifert, F., Rubie, D.C., 1997. The cubic-tetragonal phase transition in the system majorite ($\text{Mg}_4\text{Si}_4\text{O}_{12}$) - pyrope ($\text{Mg}_3\text{Al}_2\text{Si}_3\text{O}_{12}$), and garnet symmetry in the Earth's transition zone. *Physics and Chemistry of Minerals* 24, 206–221.
- Helffrich, G., Wood, B.J., 1989. Subregular model for multicomponent solutions. *American Mineralogist* 74, 1016–1022.
- Holland, T.J.B., Powell, R., 2011. An improved and extended internally consistent thermodynamic dataset for phases of petrological interest, involving a new equation of state for solids. *Journal of Metamorphic Geology* 29, 333–383.
- Huang, S., Chen, J., 2014. Equation of state of pyrope-almandine solid solution measured using a diamond anvil cell and in situ synchrotron X-ray diffraction. *Physics of the Earth and Planetary Interiors* 228, 88–91.
- Hunt, S.A., Dobson, D.P., Li, L., Weidner, D.J., Brodholt, J.P., 2010. Relative strength of the pyropemajorite solid solution and the flow-law of majorite containing garnets. *Physics of the Earth and Planetary Interiors* 179, 87 – 95.
- Komabayashi, T., 2014. Thermodynamics of melting relations in the system Fe-FeO at high pressure: Implications for oxygen in the Earth's core. *Journal of Geophysical Research (Solid Earth)* 119, 4164–4177.
- Kowalski, M., Spencer, P., 1995. Thermodynamic reevaluation of the C-O, Fe-O and Ni-O systems: Remodelling of the liquid, BCC and FCC phases. *Calphad* 19, 229 – 243.
- Nestola, F., Boffa Ballaran, T., Liebske, C., Bruno, M., Tribaudino, M., 2006. High-pressure behaviour along the jadeite $\text{NaAlSi}_2\text{O}_6$ -aegirine $\text{NaFeSi}_2\text{O}_6$

- 295 solid solution up to 10 GPa. *Physics and Chemistry of Minerals* 33, 417–425.
- Newton, R.C., Charlu, T.V., Kleppa, O.J., 1977. Thermochemistry of high pressure garnets and clinopyroxenes in the system $\text{CaO-MgO-Al}_2\text{O}_3\text{-SiO}_2$. *Geochimica et Cosmochimica Acta* 41, 369–377.
- 300 Ozawa, H., Takahashi, F., Hirose, K., Ohishi, Y., Hirao, N., 2011. Phase Transition of FeO and Stratification in Earth’s Outer Core. *Science* 334, 792–.
- Seagle, C.T., Heinz, D.L., Campbell, A.J., Prakapenka, V.B., Wanless, S.T., 2008. Melting and thermal expansion in the Fe-FeO system at high pressure. *Earth and Planetary Science Letters* 265, 655–665.
- 305 Tsuno, K., Ohtani, E., Terasaki, H., 2007. Immiscible two-liquid regions in the Fe O S system at high pressure: Implications for planetary cores. *Physics of the Earth and Planetary Interiors* 160, 75–85.